Biogeosciences, 8, 883–899, 2011
www.biogeosciences.net/8/883/2011/
doi:10.5194/bg-8-883-2011

Biogeosciences

Integrated survey of elemental stoichiometry (C, N, P) from the western to eastern Mediterranean Sea

M. Pujo-Pay[1,2], P. Conan[1,2], L. Oriol[1,2], V. Cornet-Barthaux[3], C. Falco[4], J.-F. Ghiglione[1,2], C. Goyet[4], T. Moutin[3], and L. Prieur[5,6]

[1]Laboratoire d'Océanographie Microbienne, INSU-CNRS, UMR 7621, Observatoire Océanologique, 66651 Banyuls/mer, France
[2]UPMC Univ. Paris 06, UMR 7621, Laboratoire d'Océanographie Microbienne, Observatoire Océanologique, 66651 Banyuls/mer, France
[3]Laboratoire d'Océanographie Physique et Biogéochimique (LOPB), UMR 6535, CNRS-IRD-Université de la Méditerranée, Centre d'Océanologie de Marseille, Campus de Luminy, Case 901, 13288 Cedex 09 Marseille, France
[4]UPVD, IMAGES, EA 4218, Bât. B, 52 avenue Paul Alduy, 66860 Perpignan, France
[5]Laboratoire d'Océanographie de Villefranche, INSU-CNRS, UMR 7093, Observatoire Océanologique, 06234 Villefranche/mer, France
[6]UPMC Univ. Paris 06, UMR 7093, Laboratoire d'Océanographie de Villefranche, Observatoire Océanologique, 06230 Villefranche/mer, France

Received: 22 July 2010 – Published in Biogeosciences Discuss.: 11 October 2010
Revised: 29 March 2011 – Accepted: 30 March 2011 – Published: 8 April 2011

Abstract. This paper provides an extensive vertical and longitudinal description of the biogeochemistry along an East-West transect of 3000 km across the Mediterranean Sea during summer 2008 (BOUM cruise). During this period of strong stratification, the distribution of nutrients, particulate and dissolved organic carbon (DOC), nitrogen (DON) and phosphorus (DOP) were examined to produce a detailed spatial and vertically extended description of the elemental stoichiometry of the Mediterranean Sea. Surface waters were depleted in nutrients and the thickness of this depleted layer increased towards the East from about 10 m in the Gulf of Lion to more than 100 m in the Levantine basin, with the phosphacline deepening to a greater extent than that for corresponding nitracline and thermocline depths. We used the minimum oxygen concentration through the water column in combination with 2 fixed concentrations of dissolved oxygen to distinguish an intermediate layer (Mineralization Layer; ML) from surface (Biogenic Layer; BL), and deep layers (DL). Whilst each layer was represented by different water masses, this approach allowed us to propose a schematic box-plot representation of the biogeochemical functioning of the two Mediterranean basins. Despite the increasing oligotrophic nature and the degree of P-depletion along the West to East gradient strong similarities were encountered between eastern and western ecosystems. Within the BL, the C:N:P ratios in all pools largely exceeded the Redfield ratios, but surprisingly, the nitrate vs. phosphate ratios in the ML and DL tended towards the canonical Redfield values in both basins. A change in particulate matter composition has been identified by a C increase relative to N and P along the whole water column in the western basin and between BL and ML in the eastern one. Our data showed a noticeable stability of the DOC:DON ratio (12–13) throughout the Mediterranean Sea. This is in good agreement with a P-limitation of microbial activities but in contradiction of the accepted concept that N is recycled faster than C. The western and eastern basins had similar or close biological functioning. Differences come from variability in the allochtonous nutrient sources in terms of quantity and quality, and to the specific hydrodynamic features of the Mediterranean basins.

1 Introduction

The carbon (C), nitrogen (N), and phosphorus (P) elemental composition of mineral and organic matter in marine environments is a key factor for relating carbon and nutrient cycles. Stoichiometric ratios are powerful tools to model basic

Correspondence to: M. Pujo-Pay
(mireille.pujo-pay@obs-banyuls.fr)

biogeochemical patterns of the sea. Since Redfield (1934) presented this concept of closely linked elemental ratios in the biogeochemical cycles of the ocean, it has served as one of the foundations of biogeochemical researches (Falkowski and Davis, 2004). Indeed, the nutrient ratios in the sea have been recurrently used as water mass tracers and as effective markers of biotic and of the biogeochemical processes taking place in the ocean interior (Redfield et al., 1963; Sterner et al., 2008). The canonical values proposed by Redfield (molar ratio of 105:16:15:1 in the North-Atlantic for C:N:Si:P) still hold as a reference (e.g. Arrigo, 2005). Measurements of C:N:P ratios and anomalies relative to the Redfield values are generally useful to describe the functioning of complex food webs and to examine the processes that regulate marine biogeochemistry. These anomalies have been successfully used to trace temporal changes occurring in the global ocean on a wide range of scales (e.g. Falkowski, 1997; Pahlow and Riebesell, 2000; Béthoux et al., 2002; Sarmiento and Gruber, 2006), including estimation of the global distribution of anthropogenic carbon (Gruber and Sarmiento, 1997), rate of nitrogen fixation (Deutsch et al., 2007), denitrification (Tyrrell and Lucas, 2002), and ocean mixing (Schroeder et al., 2010).

Although the scientific community has gained greater insights into elemental cycling by using the Redfield ratios, the processes that create the near constancy in elemental ratios continue to be examined (i.e. Klausmeier et al., 2008). It is known that the elemental composition of biotic and abiotic compartments can widely vary with environmental conditions (light, temperature, trophic status), or growth rate of living organisms (Hansell and Carlson, 2002; Anderson et al., 2005; Conan et al., 2007; Sterner et al., 2008). Spatial variability in elemental ratios has been reported with respect to remineralisation of organic matter changing with depth and with ambient oxygen levels (Paulmier and Ruiz-Pino, 2009).

Climate change effects are predicted to play a prominent role in modifying the Mediterranean nutrient status that can result from a direct change of the total input rates and/or alteration of nutrient stoichiometry, which will affect the microbial activity and diversity and subsequently, the whole ecosystem (Turley, 1999; Crispi et al., 2001). For example, the predicted increase in sea surface temperature combined with changes in thermohaline circulation will accentuate the thermal stratification of the surface layer which may reduce the supply of nutrients to the photic layer through vertical transport (Marty and Chiavérini, 2010). This is likely to increase the severity of oligotrophic conditions and therefore, the potential role of external inputs operating on larger timescales will become relatively more important in controlling the nutritional status of the Mediterranean Sea (for more details, see Mermex group, 2011).

The Mediterranean Sea is an elongated semi-enclosed basin with significant exchanges only at the Gibraltar strait. It is divided in two sub-basins, linked via the Sicilian strait, which has a shallow sill that helps to decouple the hydrodynamic and ecological conditions in the two sub-basins, the western and the eastern basins. The presence of these 2 shallow sills precludes a significant exchange of deep waters with the Atlantic Ocean as well as between the two Mediterranean basins. The general circulation transforms surface Atlantic Water into a set of saltier and denser typical Mediterranean Waters that are formed in different areas within the sub-basins and thus have distinct hydrological characteristics. Robinson et al. (2001) described the western basin scale thermohaline cell, as driven by deep water formed in the Gulf of Lion and spreading from there. Intense mesoscale activity exists along the coastal current, within the mid-sea eddies and along the outer rim swirl flow of a sub-basin scale gyre (Millot and Taupier-Letage, 2005). The basin scale thermohaline cell of the eastern basin is mainly composed of energetic sub-basin scale gyres linked by sub-basin scale jets. The active mesoscale processes are shown by a field of internal eddies, meanders along the border swirl flow of a sub-basin scale gyre, and as meandering jet segments (Robinson et al., 2001).

The Mediterranean Sea has long been known as a low nutrient concentration basin (Mc Gill, 1965; Krom et al., 1991) and as one of the largest nutrient-depleted area in the world (Ignatiades, 2005) though exhibiting increasing oligotrophy from west to east. Mediterranean coastal areas directly interact with the pelagic environment, since the shelves are relatively narrow. The Mediterranean response to external conditions is relatively fast compared to the other oceans (Crispi et al., 2001) and physical/ecological interactions at basin scale may have profound influence in determining the evolution of the ecosystems. Local environmental events such as wind-driven mixing, mesoscale hydrodynamical processes, river discharges (Ludwig et al., 2010) and atmospheric depositions (wet and dry) have an important role on the local fertilization (Mermex Group, 2011). The Mediterranean Sea is particularly relevant for biogeochemical studies, because literature reported anomalous values in nutrient ratios as compared to other oceanic provinces (Béthoux and Copin-Montégut, 1988; Herut et al., 1999; Kress and Herut, 2001; Ribera d'Alcalà et al., 2003; Ediger et al., 2005; Krom et al., 2005). This anomaly, though frequently explored, still represents an open issue for the understanding of the functioning of the Mediterranean Sea (see Krom et al., 2010; Mermex group, 2011). Because of the typical scales and morphology of the Mediterranean basins, nutrient ratios and the elemental partitioning in organic matter should depend on, and therefore reveal, the relevant internal processes of the sea, thus becoming a powerful tool to reconstruct its internal dynamics.

Our investigation during the BOUM cruise (July 2008) has allowed a description of the present inorganic and organic matter distribution and stoichiometry (C:N:P) along a longitudinal transect extending from the Levantine Sea (eastern basin) to the Gulf of Lion (north western Mediterranean). The first objective of this paper is then to fully detailed the matter stocks of the western and eastern Mediterranean ecosystems in a summer situation. We then point out

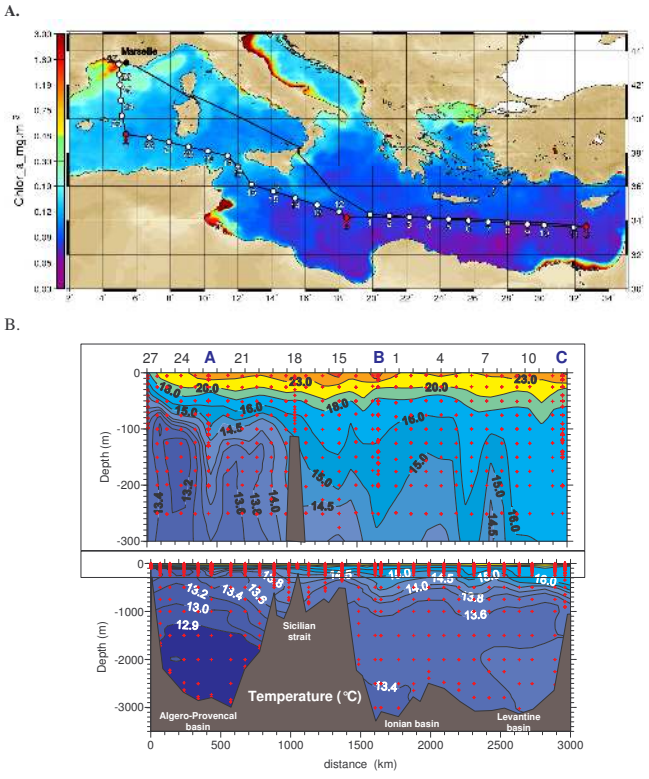

Fig. 1. **(A)** Map of the BOUM cruise transect (16 June–20 July 2008) in the Mediterranean Sea superimposed on a SeaWiFS composite image of the sea surface chlorophyll-*a* concentration (courtesy to E. Bosc). "Short duration" stations are regularly distributed and numbered from 1 to 27. The 3 "long duration (4 days)" stations A, B, and C in the western, Ionian and Levantine basins respectively are located near the centre of an anticyclonic eddy. **(B)** Vertical sections of temperature (°C) over the whole water column (bottom) and a zoom for surface (0–300 m; top). On the top x-axis, the position of the stations is indicated.

differences and similarities between the two basins in terms of C:N:P elemental partitioning. The second objective is to propose new hypothesis to reconcile the biological Mediterranean functioning with the Redfield concept.

2 Materials and methods

2.1 Study area and sampling

During the "BOUM" cruise (Biogeochemistry from the Oligotrophic to the Ultra oligotrophic Mediterranean Sea) that took place during the summer 2008 on the R/V *L'Atalante*, a transect of 30 stations from the Levantine basin to the north western Mediterranean Sea has been investigated from surface to Sea floor (Fig. 1a). Full geographical information is given in Moutin et al. (2011). The east-west cruise track crossed the main areas of the Mediterranean Sea, the Levantine basin, the Cretan passage region, the Ionian basin, and the Sicilian strait before entering the western basin and crossed the algéro-Provencal basin (Fig. 1a and b). In the western basin, there was a south-north transect from a central station (A) toward the mouth of the Rhone River in the Gulf of Lion (Fig. 1a). Profiles of temperature, conductivity, oxygen and fluorescence were performed with a SBE 911 PLUS Conductivity-Temperature Depth (CTD) system manufactured by Sea-Bird Electronics Inc. Water samples were collected from CTD casts at the 30 stations with a carousel equipped with 24 Niskin Bottles of 12 L volume. Water was sampled at 12–17 depths, from few meters above the sea floor up to the surface (0–5 m), the number of samples depending on the parameter and on the water depth.

2.2 Analysis of nutrient and particulate and dissolved organic matter

2.2.1 Nutrients

Samples for nitrate (NO_3^-), nitrite (NO_2^-) and phosphate (PO_4^{3-}) were directly collected from the Niskin bottles in 20 ml acid washed polyethylene vials. They were immediately analysed on board according to classical methods using the automated colorimetric technique (Tréguer and Le Corre, 1975; Wood et al., 1967) on a segmented flow Bran Luebbe autoanalyser II. Precision of measurements was 0.02 µM, 0.005 µM and 0.005 µM for NO_3^-, NO_2^-, and PO_4^{3-} respectively and detection limits for the procedures were 0.02 µM, 0.01 µM and 0.01 µM for NO_3^-, NO_2^-, and PO_4^{3-}, respectively. Nutrient standardisation and data quality were assured through successful and continuous participation in international intercalibration exercises. During the cruise, measurements were further verified with the use of OSIL (Ocean Scientific International Ltd) marine nutrient standards (ISO 9001 accredited). Samples for ammonium (NH_4^+) were collected in ultra cleaned glass bottles with care to avoid contamination. NH_4^+ determinations were performed on board by fluorimetry according to Holmes et al. (1999) on a fluorimeter Jasco FP-2020. Precision of measurements was 2 nM and detection limit for the procedure was 3 nM.

2.2.2 Total inorganic carbon

Samples for total inorganic carbon (C_T) were collected from the Niskin bottles in borosilicate glass bottles. They were poisoned with a saturated $HgCl_2$ solution then sealed and stored. At the end of the cruise, they were shipped to the laboratory for analysis. The measurements were performed by potentiometry using a closed cell, according to the DOE handbook of methods for Analysis of the Various Parameters of the Carbon Dioxide System in Seawater (DOE, 1994). Typical analytical precision was less than $\pm 2\,\mu mol\,kg^{-1}$. The accuracy was verified using regular measurements of reference material (CRM) bought from A. Dickson's laboratory (Scripps, USA).

2.2.3 Dissolved organic matter

Samples for dissolved organic matter (DOM) were collected from the Niskin bottles in combusted glass bottles. Samples where then immediately filtered through 2 precombusted (24 h, 450 °C) glass fiber filters (Whatman GF/F, 25 mm). Samples for dissolved organic carbon (DOC), collected into precombusted glass tubes and acidified with Orthophosphoric acid (H_3PO_4), were immediately analyzed on board by high temperature catalytic oxidation (HTCO) (Sugimura and Suzuki, 1988; Cauwet, 1994, 1999) on a Shimadzu TOCV analyzer. Typical analytical precision is ±0.1–0.5 (SD) or 0.2–1% (CV). Standardisation and data quality were assured through the successfull and continuous participation in laboratory international intercalibrations exercices. Furthermore, consensus reference materials (http://www.rsmas.miami.edu/groups/biogeochem/CRM.html) was injected every 12 to 17 samples to insure stable operating conditions. Samples for dissolved organic nitrogen (DON) and phosphorus (DOP), collected in Teflon vials, were immediately analyzed by persulfate wet-oxidation according to Pujo-Pay and Raimbault (1994) and Pujo-Pay et al. (1997).

2.2.4 Particulate organic matter

Particulate nitrogen (PN) and phosphorus (PP) were collected onto precombusted (24 h, 450 °C) glass fiber filters (Whatman GF/F, 25 mm), that were immediately oxidized after filtration into Teflon vial and simultaneously analyzed on board according to the wet oxidation procedure of Pujo-Pay and Raimbault (1994). Particulate organic carbon (POC) was collected on precombusted (24 h, 450 °C) glass fiber filters (Whatman GF/F, 25 mm). Filters were dried in an oven at 50 °C and stored, in ashed glass vial and in a dessicator until analyses when return from the cruise, on a CHN Perkin Elmer 2400.

3 Results

3.1 Hydrological characteristics

The Mediterranean Sea is divided in two main basins, the western (stations 18 to 27, and A) and eastern (stations 17 to 1, B and C) basins which are separated by the Sicilian strait (Fig. 1a). The overall circulation and the physical and hydrologic characteristics (e.g. T-S properties) of the different water masses in the Mediterranean Sea has been previously well described (see for example Robinson, 2001; or Millot and Taupier-Letage, 2005), likewise full details for the BOUM cruise can be found in Moutin et al. (2011). Briefly, in both basins, the water masses tend to follow the isobaths at their own level in the counterclockwise sense, then describing quasi-permanent gyres a few 10 s km thick and a few 1000 s km long along the continental slope. As the southern parts of both gyres are markedly unstable (Millot and Taupier-Letage, 2005), this scheme is not so simple. In addition to these circulation features, the deep water masses must be uplifted before outflowing from the various openings that are only a few 100 s m deep (Fig. 1b).

During the BOUM cruise, the highest surface temperatures ranged from 24 °C in the western basin (at station A) to 27.5 °C in the central eastern part (at station B). The deep waters temperature ranged from 12.9 to 13.0 °C in the western basin and from 13.4 to 13.6 °C in the eastern basin, with the exception of the extreme East of the Levantine part, where deep temperature approached 13.8 °C (Fig. 1b). These relatively warm deep waters (the same increase pattern is observed for salinity, not shown) are attributed to the memory of the recent change in deep water formation of the Eastern basin named the Eastern Mediterranean Transient, EMT (Robinson et al., 2001). The various anticyclonic eddies were easily identified by a local deepening of isotherms (Fig. 1b). Chlorophyll concentration showed a well defined Deep Chlorophyll Maximum (DCM), more pronounced in the western basin (for details, see Crombet et al., 2011), and deepening from west (∼40 to 80 m) to east (from 80 to >100 m).

3.2 Evolution of biogeochemical parameters

3.2.1 Division of the water column

In order to describe and to analyze the BOUM transect, we chose to differentiate three successive vertical layers in both basins (Fig. 2a). The principle of a fixed depth is obviously not appropriate in considering the vertical and latitudinal variability and evolution of the parameters described hereafter. Our idea comes from the fact that particulate organic matter (POM) synthesizes in the euphotic layer could sink to be mineralized in depth with a consumption of oxygen. This process occurs both in the western than in the eastern basin and is partly independent of water masses. The oxygen concentration could be then considered as representative of the balance between water mass mixing and biological mineralization processes. We have considered the depth of the minimum in oxygen concentration to define the core of the mineralization layer. We have then fixed 2 limits (up and down) of this layer by 2 different concentrations in dissolved oxygen to separate a surface layer, and a deep layer. The 3 defined layers could be composed by different water mass type but the "composite" water masses should have weak density variation along the east-west transect.

Using this distinction, the intermediate layer, named hereafter "Mineralization Layer (ML)" includes the minimum oxygen concentration, generally associated with the highest nutrient concentrations in the case of the Oxygen Minimum Zones (OMZs; Paulmier and Ruiz-Pino, 2009). The upper limit of this ML is fixed when oxygen concentration reaches 195 µmol kg^{-1} (Fig. 2a). Then, the layer from the surface to that depth corresponds to the "Biogenic Layer

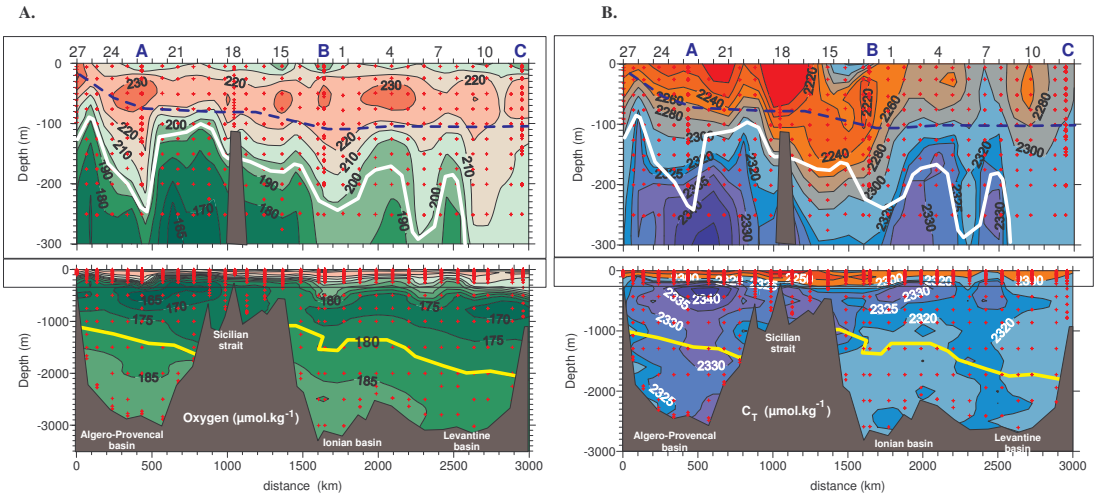

Fig. 2. Surface (top) and total water column (bottom) vertical sections of **(A)** oxygen concentration and **(B)** Carbon inorganic total concentration (C_T) along the BOUM transect. The white full line in surface section illustrates the limit of 195 µmol kg^{-1} in oxygen between the Biogenic Layer (BL) and the Mineralization Layer (ML). The blue dashed line follows the depth of the deep chlorophyll maximum (full section is presented in Crombet et al., 2011). The yellow full line in the deep section illustrates the limit of 180 µmol kg^{-1} in oxygen between the ML and the Deep Layer (DL). See text for further explanation. On the top x-axis, the position of the stations is indicated.

(BL)". This BL includes the DCM, just below a relative maximum in dissolved oxygen concentration (Fig. 2a). The lower limit of the ML is fixed when oxygen concentration reaches 180 µmol kg^{-1}. The layer below that depth until the sea floor corresponds hereafter to the "deep layer (DL)". The thickness of these 3 layers varies from station to station, but the relevance of this delimitation is confirmed by the distribution of the total inorganic carbon (C_T) along the transect (Fig. 2b). Indeed, ML encompasses the relative maximum in C_T concentrations (>2330 µmol kg^{-1}), whereas BL are characterized by the lowest concentrations (<2300 µmol kg^{-1}) and DL by homogenous concentrations (∼2320–2325 µmol kg^{-1}).

3.2.2 Dissolved inorganic matter

In BL, concentrations of nitrate+nitrite ($NO_3^- + NO_2^-$), NO_2^- and PO_4^{3-} are low and close or below the detection limit of conventional micromolar technology (Fig. 3a). In this layer, concentrations of C_T are also minimal with 2315 ± 47 µM in the western basin and 2334 ± 47 µM in the eastern basin (Table 1). Concentrations of NH_4^+ are also low (0–10 nM) with a patchiness pattern and maxima in subsurface, similarly to NO_2^- distribution with a peak (max values about 0.2 µM) at the basis of the DCM (Figs. 2, 3b and Table 1). Below this depleted nutrient layer, concentrations rise through the nutriclines and reach maximal values of about 9.8, 0.09, 0.055 and 0.44 µM in the western basin and of about 6.3, 0.22, 0.056 and 0.25 µM in the eastern basin for $NO_3^- + NO_2^-$, NO_2^-, NH_4^+ and PO_4^{3-}, respectively. Below these maxima (located in BL for NO_2^- and NH_4^+ but in the ML for $NO_3^- + NO_2^-$ and PO_4^{3-}), nutrient concentrations slightly decrease to reach ∼9.4 and ∼0.42 µM in the western basin and ∼5.6 and ∼0.20 µM in the eastern basin for $NO_3^- + NO_2^-$ and PO_4^{3-} respectively in DL (Fig. 3c and Table 1). Within the two deep layers, the average concentrations of C_T are close (i.e., 2394 ± 7 µM and 2387 ± 4 µM in DL for western and eastern basins, respectively), while both the minimum and maximum concentrations are located in the western basin (Fig. 2b and Table 1).

In the western part of the Sicilian strait, the shape of the various isolines changes (station 18) and a nutrient anomaly characterized by lower concentrations is encountered near 1000 m in the western basin, where concentrations are ≤0.3 µM of PO_4^{3-} and ≤5.5 µM of $NO_3^- + NO_2^-$ as compared to average western values at the same depth (∼0.40–0.45 µM of PO_4^{3-} and 9.0–9.5 µM of $NO_3^- + NO_2^-$) (Fig. 3c). A similar pattern is shown for concentrations in C_T (Fig. 2b). This characterizes the flow of subsurface eastern waters to the western basin.

The thicknesses of the nutrient depleted layer changes along the west-east transect from 10–20 m in the Gulf of Lion to more than 100 m in the Levantine basin. Taking into account the bias introduced by discrete sampling, the upper limit of the nitracline is close to the basis of the thermocline (see legend of Fig. 4 for definition). The top of the phosphacline is generally located deeper than the top of the nitracline, above the basis of the thermocline in the western basin but below it in the eastern one (Fig. 4). The discrepancy between the two nutriclines increases eastward as the phosphacline deepens more rapidly than the nitracline and the thermocline. It is important to note that we have considered a threshold in the gradient to define the top of the nutriclines. When the nitracline and the phosphacline are separated with depth, low

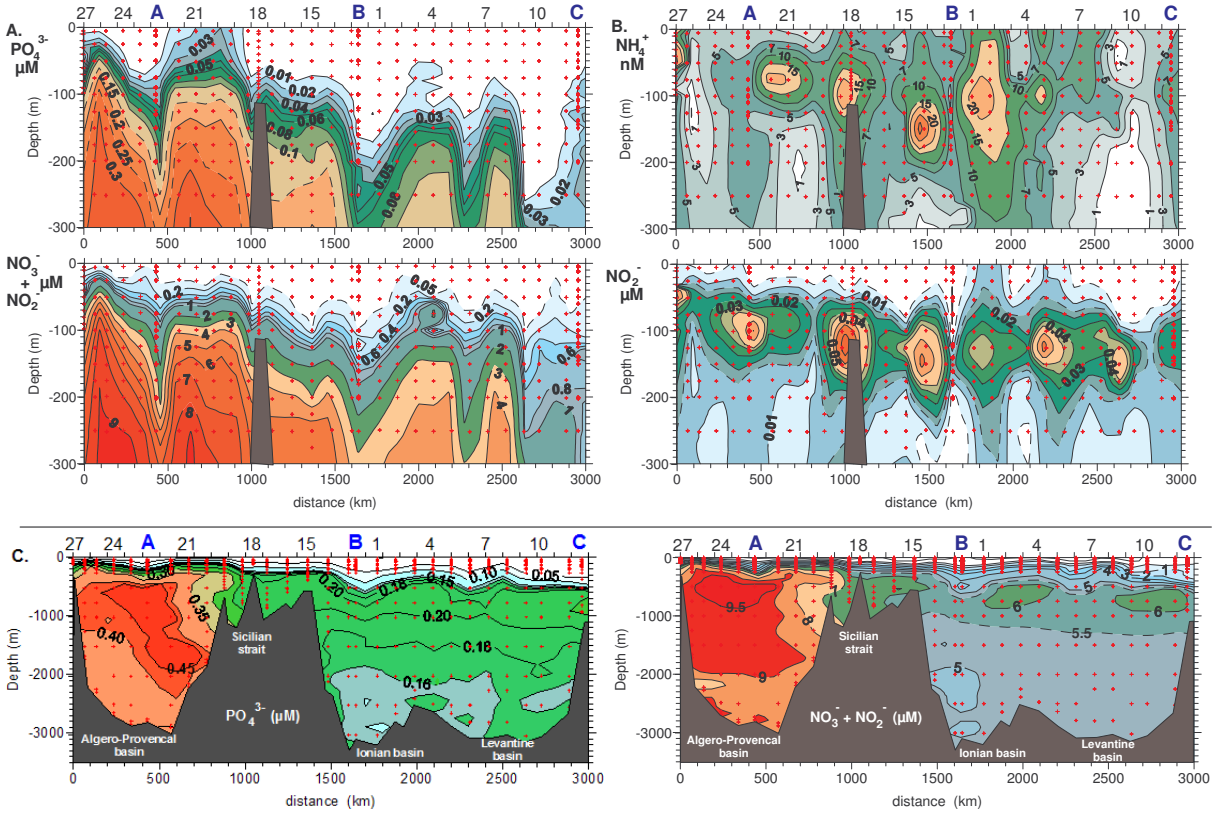

Fig. 3. Surface (0–300 m) vertical sections of **(A)** phosphate (PO_4^{3-}), nitrate + nitrite ($NO_3^- + NO_2^-$), and **(B)** ammonium (NH_4^+) and nitrite (NO_2^-) along the BOUM transect. **(C)** as in **(A)** for the whole water column. On the top x-axis, the position of the stations is indicated.

concentrations of PO_4^{3-} could be measured in the gap (concentration $<0.08\,\mu M$) but the vertical gradient is then insufficient to meet our criteria.

3.2.3 Dissolved (DOM) and particulate (POM) organic matter, and elemental partitioning

In BL, dissolved organic phosphorus (DOP), carbon (DOC) and nitrogen (DON) show different distribution patterns (Fig. 5a). Indeed, DOC concentration roughly follows an inverse distribution compared to nutrient, with maxima in surface waters and an increase from west (69.4 µM) to east (72.4 µM). For both DON and DOP, maximal concentrations are also measured in the surface waters (Table 1), but highest values are encountered in the central part of the transect (at station B in the eastern basin). The two basins have similar mean DON concentration in BL ($\sim 4.7 \pm 0.6\,\mu M$) whereas the western basin is slightly richer in DOP ($0.06 \pm 0.02\,\mu M$) than the eastern one ($0.04 \pm 0.02\,\mu M$). Below BL, a steep gradient is encountered for DOM (i.e. for DOC, DON and DOP) and fairly homogeneous concentrations follow with depth (Fig. 5b). The whole water column is not shown for DOP, because according to the station, DOP concentration is undetectable below 150 to 500 m in the western basin and below 200 to 750 in the eastern basin. Contrary to nutrient, DOM distribution in DL does not reveal significant gradient between the western and eastern basins (Fig. 5b). Average DOC and DON concentrations in DL are $39.9 \pm 1.1\,\mu M$, $3.3 \pm 0.4\,\mu M$ for the western basin and $41.1 \pm 1.4\,\mu M$, $3.1 \pm 0.5\,\mu M$ for the eastern basin (Table 1).

For both basins, C_T represents more than 97% of the total carbon pool in surface waters, whereas DOC and POC represent about 2.5 and 0.1%, respectively (Table 2). For the N and P pools, differences are encountered between western and eastern basins: In the western BL, nitrogen pool is composed of ~25, 70 and 5% of dissolved inorganic nitrogen (DIN), DON and PN, respectively. Phosphorus pool is composed by 40, 40 and 20% of PO_4^{3-}, DOP and PP, respectively. In the eastern BL, nitrogen pool is composed by 10, 85 and 5% of DIN, DON and PN and phosphorus pool by 15, 60 and 25% of PO_4^{3-}, DOP and PP (Table 2). The surface west-east oligotrophic gradient is clearly characterized by a decrease in the proportion of mineral to organic forms for N and P. Indeed, the organic form (dissolved + particulate) represents about 76% in N and 63% in P in the western basin to reach 92% in N and 74% in P in the eastern basin. This gradient is also characterized by a general decrease in POM (POC, PN, and PP) along the transect (Fig. 6). The

Table 1. Mean physical characteristics and chemical content of the "Biogenic Layer (BL)", "Mineralization Layer (ML)" and "Deep Layer (DL)" for the western and eastern basins of the Mediterranean Sea during the BOUM cruise. The standard deviations (σ), as well as minimal and maximal values ([min–max]), are indicated for each variable. "Pot. Dens. Excess" is for potential density excess relative to 0 dbars.

		Western basin			Eastern basin		
		mean	σ	[min–max]	mean	σ	[min–max]
BL							
Depth	m	56	43	[0–150]	85	56	[0–250]
Potential T	°C	17.20	4.15	[13.12–25.12]	17.91	2.99	[15.03–26.77]
Salinity		38.05	0.29	[37.30–38.44]	38.61	0.53	[37.29–39.44]
Pot. Dens. excess	$kg\,m^{-3}$	27.74	1.19	[25.05–29.03]	28.03	0.93	[14.79–29.10]
O_2	µM	227	18	[200–261]	224	13	[200–247]
C_T	µM	2315	47	[2228–2391]	2334	42	[2221–2395]
PO_4^{3-}	µM	0.05	0.06	[0–0.17]	0.01	0.02	[0–0.11]
$NO_3^- + NO_2^-$	µM	1.56	2.19	[0–5.84]	0.56	0.88	[0–3.45]
NO_2^-	µM	0.020	0.025	[0–0.088]	0.023	0.033	[0–0.215]
NH_4^+	µM	0.007	0.012	[0–0.055]	0.008	0.008	[0–0.056]
DOC	µM	58.7	7.4	[45.3–69.4]	61.5	5.9	[49.4–72.4]
DON	µM	4.7	0.4	[4.1–5.5]	4.7	0.6	[3.5–6.3]
DOP	µM	0.06	0.02	[0.02–0.09]	0.04	0.02	[0.01–0.10]
POC	µM	4.31	1.73	[1.45–8.70]	3.08	0.90	[0.80–5.41]
PN	µM	0.45	0.17	[0.14–0.87]	0.30	0.11	[0.08–0.66]
PP	µM	0.022	0.009	[0.010–0.045]	0.014	0.005	[0.004–0.030]
ML							
Depth	m	420	352	[75–1250]	500	309	[150–1250]
Potential T	°C	13.43	0.32	[12.91–14.06]	14.17	0.54	[13.54–15.16]
Salinity		38.50	0.12	[38.11–38.70]	38.83	0.08	[38.67–39.01]
Pot. Dens. excess	$kg\,m^{-3}$	29.02	0.12	[28.58–29.11]	29.11	0.09	[28.79–29.19]
O_2	µM	181	8	[167–195]	186	9	[174–195]
C_T	µM	2395	10	[2361–2412]	2388	16	[2319–2405]
PO_4^{3-}	µM	0.33	0.07	[0.15–0.44]	0.17	0.05	[0.04–0.25]
$NO_3^- + NO_2^-$	µM	8.03	1.42	[4.64–9.81]	5.16	1.00	[2.82–6.30]
NO_2^-	µM	0.010	0.005	[0–0.024]	0.010	0.008	[0–0.032]
NH_4^+	µM	0.001	0.002	[0–0.007]	0.002	0.004	[0–0.023]
DOC	µM	42.9	3.8	[37.6–53.3]	44.0	4.3	[37.5–54.1]
DON	µM	3.5	0.4	[2.5–4.1]	3.5	0.6	[2.1–5.4]
DOP	µM	0.01	0.02	[0–0.06]	0.01	0.02	[0–0.07]
POC	µM	1.35	0.28	[0.82–1.83]	1.27	0.28	[0.70–1.96]
PN	µM	0.12	0.04	[0.03–0.22]	0.08	0.04	[0.01–0.21]
PP	µM	0.009	0.005	[0.001–0.020]	0.006	0.003	[0.001–0.013]
DL							
Depth	m	1875	553	[1000–2900]	2000	528	[1000–3000]
Potential T	°C	12.89	0.03	[12.86–12.98]	13.54	0.07	[13.40–13.64]
Salinity		38.48	0.01	[38.46–38.49]	38.76	0.02	[38.72–38.79]
Pot. Dens. excess	$kg\,m^{-3}$	29.11	0.00	[29.11–29.12]	29.19	0.01	[29.18–29.2]
O_2	µM	190	4	[182–195]	188	3	[183–193]
C_T	µM	2394	7	[2377–2404]	2387	4	[2378–2395]
PO_4^{3-}	µM	0.39	0.02	[0.37–0.42]	0.17	0.01	[0.14–0.20]
$NO_3^- + NO_2^-$	µM	9.05	0.22	[8.60–9.44]	5.14	0.19	[4.80–5.64]
NO_2^-	µM	0.007	0.003	[0–0.013]	0.008	0.011	[0–0.047]
NH_4^+	µM	nd	nd	nd	nd	nd	nd
DOC	µM	39.9	1.1	[37.9–41.9]	41.1	1.4	[38.4–43.9]
DON	µM	3.3	0.4	[2.9–4.3]	3.1	0.5	[2.1–4.0]
DOP	µM	0.01	0.01	[0–0.03]	0.02	0.02	[0–0.07]
POC	µM	1.21	0.37	[0.74–1.80]	1.12	0.33	[0.80–2.03]
PN	µM	0.06	0.03	[0.01–0.13]	0.07	0.03	[0.01–0.13]
PP	µM	0.004	0.003	[0.001–0.010]	0.005	0.002	[0.001–0.008]

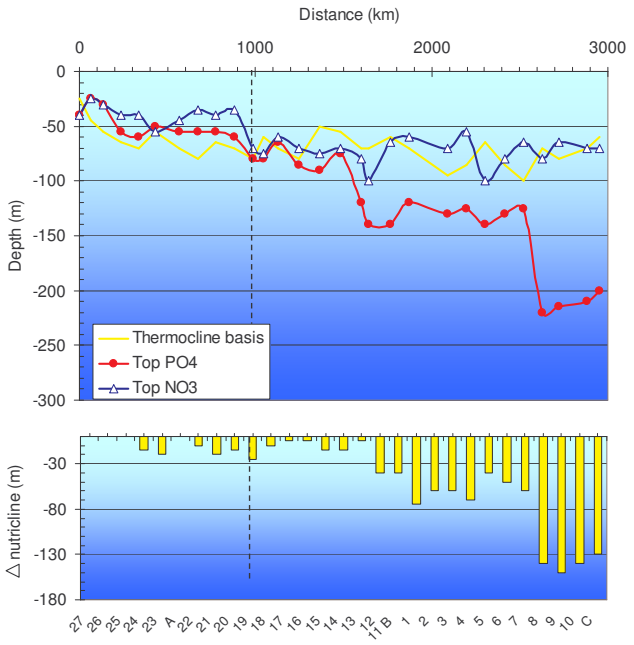

Fig. 4. Evolution of the depth of the thermocline basis, and the top of the nitracline and phosphacline along the BOUM transect. The vertical dashed line separates the western and the eastern basins. On the x-axis, the position of the stations is indicated. The thermocline basis for temperature and the top for the nutriclines are defined for the depth where the difference in concentration or temperature between two successive depths exceeds a threshold of 0.05 and 0.02 for NO_3^- and PO_4^{3-} respectively, or fall under a threshold of 0.4 for temperature. The histogram shows the difference between the depths of the nitracline and phosphacline along the transect.

highest concentrations are measured in the western basin above 100 m (8.70 µM, 0.87 µM, and 0.045 µM for POC, PN, and PP, respectively). The Gulf of Lion is the richest area but high concentrations are also measured close to the Sicilian strait and in the central part of the Ionian Sea. As compared to the hydrological structure, the POM distribution is not characterized by a west-east deepening of isolines. Below 100 m, the importance of POM as a reservoir of C, N and P declined with depth, concomitantly to the rise of the contribution of the dissolved inorganic reservoir. In terms of C and P in DL, the inorganic form represents 98% and the organic forms account for only 2%. The N proportion is 70% in DIN and 30% in DON in the western basin, and 60% in DIN and 40% in DON in the eastern basin due to a lesser content in DIN (Table 2).

3.2.4 Evolution along the Mediterranean transect

Our set of parameters could be divided in three groups characterized by different patterns along the East-West transect (Fig. 7). On an aerial approach (i.e. in considering the integrated quantity in the BL), temperature, salinity, density, dissolved oxygen, C_T, DOC and DON show a relative increase eastward (Fig. 7a), whereas $NO_3^- + NO_2^-$ and PO_4^{3-} decrease (Fig. 7b). The others parameters (NO_2^-, NH_4^+, DOP, POC, PN, PP) show no clear gradient (Fig. 7c).

4 Discussion

This study documents a west-east transect across the Mediterranean Sea, showing the succession from oligotrophic to ultra-oligotrophic regimes encountered during the summer stratified condition. The examination of chemical pools in marine environments rarely considers the three components (dissolved inorganic, dissolved organic and particulate) simultaneously through the whole water column. As a consequence, our knowledge on the partitioning of matter among these pools is relatively poor, particularly in the Mediterranean Sea. This study contributes to bridge this gap and to unravel the various inferences from the nutrients recycling and their possible role as limiting factor for primary production and mineralization.

4.1 Characterization of the Mediterranean pelagic ecosystem during stratified condition and possible evolution

During the summer, a strong thermocline was ubiquitous throughout the Mediterranean Sea (D'Ortenzio and Ribera d'Alcala, 2009). The DCM deepened with the increasing trend in oligotrophy eastward. The presence of a prominent nitrite maximum (PNM) at the basis of the DCM has been ascribed by some authors to an incomplete assimilatory reduction of nitrate by phytoplankton (phytoplankton excretion), with chemoautotrophic oxidation of ammonium by nitrifying bacteria playing only a supporting role (Lomas and Lipschultz, 2006). Biological and physical interactions are also likely to be important in controlling PNM formation and maintenance. The presence of low but measurable ammonium in the photic zone suggests that grazing was a non negligible process since ammonium is the first product of microbial grazing, which is then rapidly recycled through bacterial and phytoplankton production (Thingstad et al., 2005).

Since microorganisms have a capacity for rapid growth, they are a major component of global nutrient cycles (Arrigo, 2005). At very low nutrient concentration, DOM could accumulate (i.e. production exceed consumption and export) in the surface waters suggesting that recycling processes were limited by nutrient availability (Pujo-Pay and Conan, 2003), particularly in P in the Mediterranean Sea (Van Wambeke et al., 2002; Lucea et al., 2003). In the case of P-limitation of growth it is possible that DOC and DON could accumulate, whereas only DOC accumulates during N-limitation (Conan et al., 2007). Our present results show that there was an accumulation of DOC, and to a lesser extent of DON in the BL as the oligotrophic status increased, particularly in the eastern

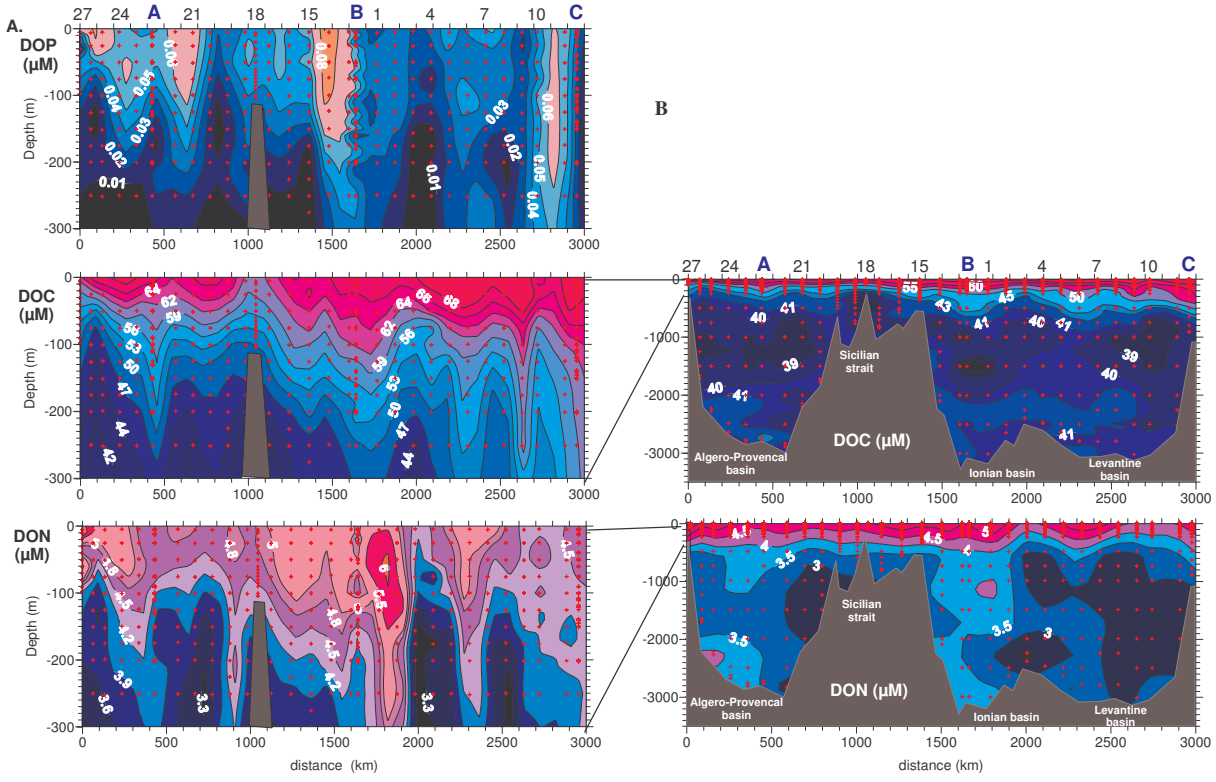

Fig. 5. Surface (0–300 m) vertical sections of **(A)** dissolved organic phosphorus (DOP), carbon (DOC), and nitrogen (DON) along the BOUM transect. **(B)** as in **(A)** for the whole water column, except for DOP which is undetectable in deep water. On the top x-axis, the position of the stations is indicated.

Table 2. Proportion (%) in C, N, P in the various compartments, inorganic, dissolved organic and particulate for the upper mixed layer (UML) and below 1000 m, in the western and eastern basins. ns means weak contribution of POM in deep waters.

	Western basin		Eastern basin	
	Surface	> 1000 m	Surface	> 1000 m
C_T	97.3±0.2	98.4±0.1	97.3±0.2	98.3±0.1
DOC	2.5±0.2	1.6±0.1	2.6±0.1	1.7±0.1
POC	0.2±0.1	ns	0.1±0.1	ns
DIN	24±8	73±2	9±4	62±4
DON	69±7	27±2	86±5	38±4
PN	7±2	ns	6±1	ns
DIP	37±9	98±2	16±9	98±4
DOP	46±7	2±2	59±7	2±4
PP	17±4	ns	25±4	ns

basin. No such tendency was observed for DOP. Vertical trends in DOC and DON have been interpreted elsewhere as a result of nutrient limited phytoplankton production, continuing to fix carbon after running out of N and/or P. Krom et al. (2005) have reported that DOC and DON contents in the surface of eastern Mediterranean waters was as high as for other oceanic areas, despite the fact that primary productivity levels were much lower. Our measurements extend these observations to include the study of phosphorus for the whole of the Mediterranean, with concentrations ranging between 38–72, 3.0–6.5, and 0–0.1 µM for DOC, DON and DOP, respectively. These values are in the range of average oceanic values given in Hansell and Carlson (2002), i.e. 35–90, 1.5–7.5, 0–0.4 µM for DOC, DON and DOP.

The downward fluxes of organic matter play a major role in sustaining and stabilizing the degree of oligotrophy observed (Crispi et al., 2001). In the present study, POC and PON represented a minor percentage of total organic C and N throughout the water column, and most of the organic matter (>80%) was present as DOC and DON as previously observed for other oligotrophic waters (Béthoux and Copin-Montégut, 1988; Vidal et al., 1999). There was a systematic decrease with depth in POM concentration reflecting the progressive decomposition of labile organic matter by bacterial consumption and respiration. In oligotrophic areas, particle flux is generally low, but strongly reacts to localized and episodic mesoscale phenomena. This flux is not necessary coupled with respect to surface ocean primary production (Lutz et al., 2002). Nevertheless, the estimation of fast sinking rates (Patara et al., 2009) is an evidence of the biological pump efficiency to sequester organic matter from the surface

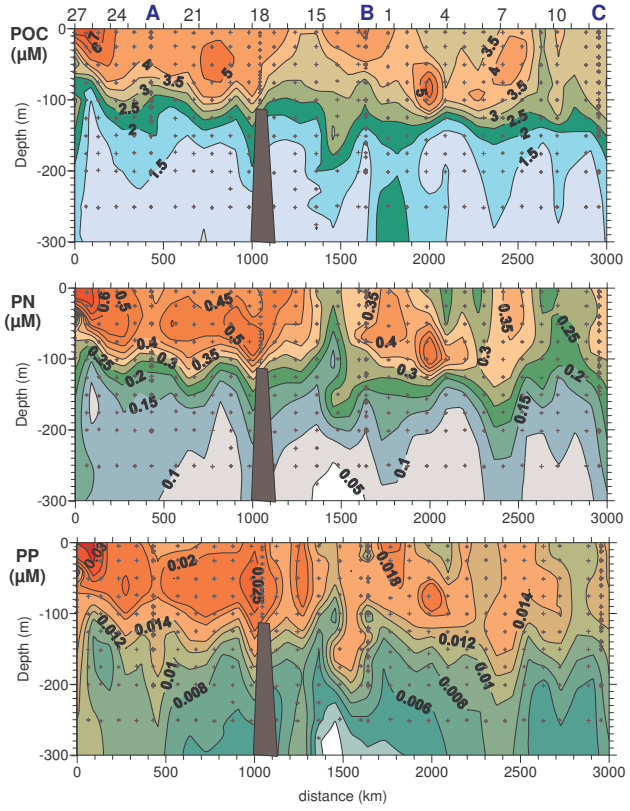

Fig. 6. Surface (0–300 m) vertical sections of particulate organic carbon (POC), nitrogen (PN) and phosphorus (PP) along the BOUM transect (deep sections not shown). On the top x-axis, the position of the stations is indicated.

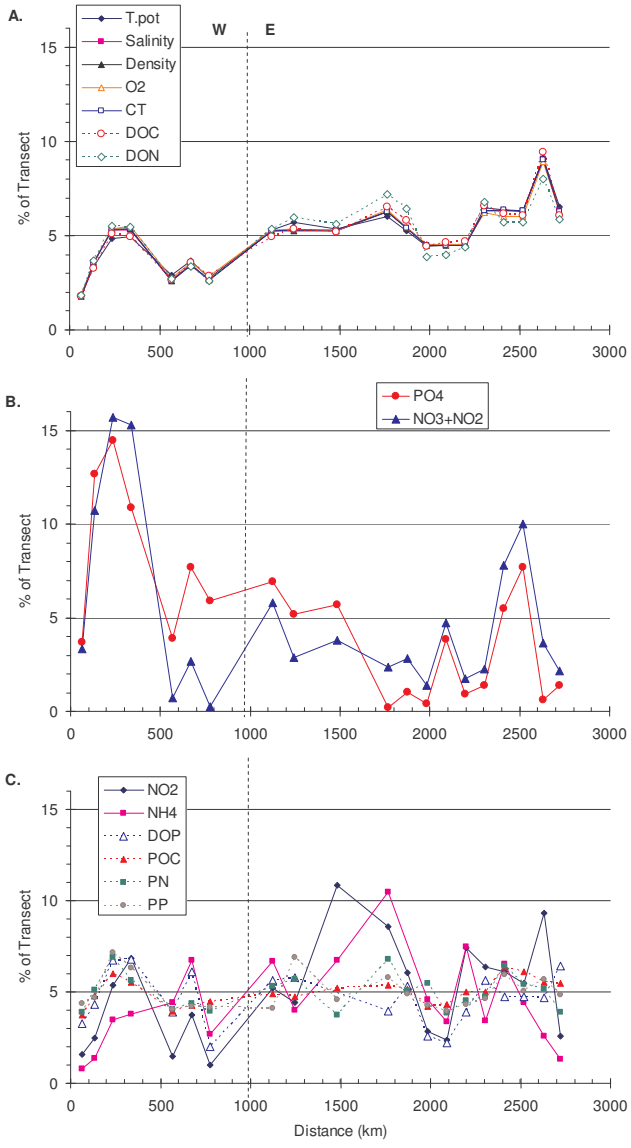

Fig. 7. Evolution of the integrated quantities within the BL, expressed at each station as the percentage along the W-E transect. **(A)** Parameters showing an increase gradient from west to east. **(B)** Parameters showing a decrease gradient from west to east. **(C)** Parameters showing no clear gradient.

layer of the eastern Mediterranean basin, but also in the western basin. In addition to this POM flux, the non-negligible downward DOM fluxes to the deep water (e.g. Vidal et al., 1999; Pujo-Pay and Conan, 2003), render this fraction as an important link between the BL, ML and DL layers, at least for C and N.

In contrast to the relative homogeneity observed in the BL of the two basins, the deep nutrient distributions showed a net transition occurring at the Sicilian strait, between a "richer" western basin and a "poorer" eastern one (Schroeder et al., 2010). The shape of the various isolines in the Sicilian strait illustrates the westward passage of the Eastern Overflow Water (EOW), cascading down to the strait in western deep waters (Millot et al., 2006), with its chemical signature clearly indicating nutrient depletion. Krom et al. (2010) recently discussed the build-up of high N:P ratios in eastern deep waters, prior to export via the Sicilian strait. These authors concluded that this exported water has a lower N:P ratio than the eastern Mediterranean deep water (EMDW) due to the preferential P-regeneration compared to N-regeneration. These exchanges (west-east in surface and east-west deeper) are of great importance in the Mediterranean-Atlantic nutrient flux exchanges because EOW comprises a fraction of waters which flow into the Atlantic through the Gibraltar strait. Moreover, Millot et al. (2006) demonstrated that outflows through the various Mediterranean straits have been continually changing during the last two decades.

The functioning of the western basin could be impacted not only by changes in surface nutrient sources (Conan et al., 2011) but also by changes in deep nutrient concentration. In theory, the elemental ratios in the deep ocean can only change on timescales comparable to residence times of the major nutrients ($\sim 10^4$ yr for NO_3^- and PO_4^{3-}, Falkowski and Davis, 2004) but the Mediterranean Sea is characterized

by very short ventilation and residence times (∼70 yr) when compared to the other oceans (500–1000 yr). Winter time mixing throughout the water column could then rapidly impact the BL, by alteration of the deep water characteristics (see for example in the Ligurian Sea; Marty and Chiavérini, 2010). An illustration of such alteration was observed in the 1990s in the eastern basin after the Eastern Mediterranean Transient (EMT) event (Klein et al., 2003; Roether et al., 2007). Indeed, the intrusion of the dense Aegean waters in the EMDW has initiated modifications in the hydrology, dynamics, chemical structure, and in some biological parameters of the entire basin (Robinson et al., 2001). Oxygen-poor, nutrient-rich waters were brought closer to the surface, enhancing the biological production in some regions after winter mixing. From 1991, a distinct intermediate layer was identified in the south Aegean, characterized by temperature, salinity and oxygen minima, and nutrient maxima. Finally, the variability in the intermediate waters can alter the preconditioning of dense water formation in the Adriatic as is possible in the western basin.

4.2 How to explain differences in the nitracline and phosphacline depths?

The development of a defined nitracline and phosphacline are frequently observed through the summer towards the basis of the upper mixed layer with the phosphacline frequently occurring below the nitracline. The depth of each of these layers increase progressively until stratification is compromised due to increased in wind-mixing and decreased solar heating (Lefèvre et al., 1997). This temporal pattern of development and relative position is also observed on a spatial scale along our longitudinal transect (Fig. 4) and becomes increasingly more prominent towards the east. The observed mesoscale variability (oscillation from station to station) is due to hydrodynamic features such as internal waves, upwelling, fronts and/or eddies (Prieur and Sournia, 1994; Pujo-Pay and Conan, 2003).

The resulted unusually high DIN:DIP ratios suggest incomplete nitrate utilization by phytoplankton due to the lack of phosphate at the bottom of the photic layer (discussed in Diaz and Raimbault, 2000). It is generally accepted that in such systems, biological consumption and subsequent export and remineralisation of nutrients in the upper ocean determine their vertical distribution (Crispi et al., 2001; Anderson et al., 2005). The consumption of nutrient to support planktonic production exhausts the surface sea layer and leads to oligotrophic conditions. This demand also generates the vertical concentration gradient driving an upward flux of dissolved inorganic nutrients previously regenerated in deeper waters (Arrigo, 2005; Schroeder et al., 2010). The position of the thermocline is usually a major determinant of the position and sharpness of nutrient gradients (Conan et al., 1999). The increasing discrepancy between the two nutriclines encountered toward the east during our study is consistent with the oligotrophic gradient and is a result of the development of spring bloom conditions in an east to west direction (D'Ortenzio and Ribera d'Alcala, 2009). In the Levantine basin, the distance between phosphacline and nitracline/thermocline is at its greatest (∼130 m). The literature has previously reported such differences in the eastern basin: 300–400 m in the south-eastern Ionian Sea (Klein et al., 2003) or 600 m in the Levantine Basin (Ediger and Yilmaz, 1996).

Krom et al. (2005) considered that the discrepancy between the depths of the phosphacline and nitracline in the Levantine basin could be due to the relative sensitivity of methodological procedures employed. In their study, sensitive (nanomolar) technology was used for both phosphate and nitrate at only one station in the Cyprus eddy, whereas at other stations, less sensitive procedures (micromolar) were deployed for determination of nitrate, with the implication that at times nitrate may have been present albeit at concentrations below the methodological limit of detection. It is necessary to investigate more intensively this point during further studies and on a larger spatial scale.

4.3 Is the Redfield ratio valuable at basin scale for the Mediterranean Sea?

The stoichiometry reflects the interaction of multiple processes, including the acquisition of the elements by plankton and/or bacteria, mineralization of organic matter by bacteria, as well as various processes of nutrient loss (burial in the sediments, outgassing to the atmosphere...) or transformation (Zehr and Ward, 2002; Sarmiento and Gruber, 2006). It is well known that nutrient supply sets an upper limit to the biological production, but planktonic organisms exert a tight control on the elemental distribution (Arrigo, 2005), affecting the chemical composition of both DOM and POM (Redfield et al., 1963). The "Redfieldian" values could be achieved when cell growth is at optimum conditions and nutrient-sufficient (Geider and La Roche, 2002). During nutrient limitation or starvation, an offset in the C:N:P ratios is observed in both nutrient uptake and in newly formed DOM, though large variability exists in and between species (Conan et al., 2007). For example, some photoautotrophic organisms can store C as lipid or carbohydrate under N and/or P limitation (Karl et al., 2001), thereby increasing their C:N and C:P ratios. The stoichiometry could also be directly impacted by the increase of C_T in seawater or indirectly by successive changes in the quantity and quality of organic matter (Mermex group, 2011). In green algae this increase can lead to higher protein content and cellular N quotas whereas in diatoms, it increases the C:P and N:P ratios and decreases the C:N ratios.

There are two different approaches to study the elemental stoichiometry as already pointed out by Kress and Herut (2001). We can consider the average ratios over depth and/or distance of the concentration of two elements, or the

Table 3. C:N:P stoichiometry expressed as the slope and the intercept (b value) of the element-element regression line and the average ratio of measured concentrations in the western and eastern basins of the Mediterranean Sea and for pooled data during the BOUM cruise. To avoid infinitive ratios, we excluded data with concentration below the detection limit. N + N is used for $NO_3^- + NO_2^-$.

	Western basin			Eastern basin			Pooled data		
	Slope	b value	ratio	Slope	b value	ratio	Slope	b value	ratio
$N+N:PO_4^{3-}$	22.9	0.3	24.5	27.9	0.3	37.8	23.3	0.6	32.4
$C_T:PO_4^{3-}$	230	2315	27 036	232	2344	89 237	169	2344	65 432
$C_T:N+N$	9.6	2315	4982	9.9	2335	4901	7.9	2337	4931
DON:DOP	20.9	3.5	162.7	15.2	3.8	160.8	17.3	3.7	161.4
DOC:DOP	284	41	1941	132	50	2055	189	47	2019
DOC:DON	8.9	12.4	12.1	8.1	18.8	13.0	8.4	16.6	12.7
PN:PP	20.7	0	19.8	18.8	0	18.8	19.6	0	19.2
POC:PP	163	0.4	256	116	1.0	235	137	0.8	243
POC:PN	8.1	0.6	13.3	5.4	1.1	14.0	7.3	0.7	13.8

equation ($y = ax + b$) of the linear relationship between these two elements in a property-property plot. Note that Redfield (1934) in his original approach used both possibilities. It is worth mentioning that the interpretation for both approaches is different (Ribera d'Alcalà et al., 2003) but complementary and can help for interpretation of the various processes involved in the relationship. Both ratios coincide if the regression line passes through the origin in the case of "ideal" (non-fractioned) nutrient co-variation (Fanning, 1992). The ratio of the net reaction rates involving N and P in each one is then equal to its concentration ratio and organisms are in balance with their environment. However, we often observe linear N:P regressions with non-zero intercepts (positive or negative), which could become quite large in the surface water layers. The term b in the linear regression equation indicates an excess (positive intercept) or a lack (negative intercept) of one element relative to the other.

We applied these two approaches to our summer data (Table 3). In the mineral pool, the excess of carbon and the increase from west to east compared to N and P is shown by high ratios. Yet, the values of the slopes and intercepts are close between western and eastern basins (~8 for $C_T:NO_3^- + NO_2^-$ and ~169 for $C_T:PO_4^{3-}$ for pooled data). The average $NO_3^- + NO_2^-:PO_4^{3-}$ ratio increases from west (24.5) to east (37.8), which can be compared to slope values (from property-property plot) of 22.9 and 27.9 for western and eastern basins, respectively (Table 3 and Fig. 8a and b). The intercepts indicate a concentration of 0.3 µM of nitrate when phosphate is exhausted for both basins (0.6 for pooled data, Fig. 8c). Such high N:P and intercepts are not uncommon and have been previously reported (Krom et al., 1991; Kress and Herut, 2001; Crispi et al., 2001). These authors also described a seasonality of the intercept values (between −0.04 and 0.73 µmol kg^{-1} in Kress and Herut, 2001) with highest values in winter, lowest values at the end of summer and intermediate values in spring and summer. It is also obvious that the coefficients of the regressions (slope and intercept) vary in the different layers (Fig. 8). Indeed, in excluding values in BL (i.e. where nutrient concentrations are low), the average ratio is still high (27.7), the excess of nitrate increase (2.1 µM), but the slope of the regression falls to a value of ~17–18 surprisingly close to the Redfield ratio, and similar for the two basins.

Kress and Herut (2001) evoked the possibility that the significance of the linear N:P relationship could be due to the large number of observations and spoke about non-linear parts for low and high phosphate concentrations. They separate their data and found a slope of 23.6 with a higher intercept value in their transition layer. In fact, the water mass distinction used in their study included some low nutrient concentrations (Fig. 8e), and partly explains the difference observed between ours and their results. The same remark could be applied in the western basin for the data compiled by Schroeder et al. (2010), who found a slope of ~19 in excluding the 0–100 m surface layer (Fig. 8d). Moreover, our data were acquired during one summer cruise as opposed to the large data set used by Kress and Herut (2001) or Schroeder et al. (2010). Consequently, the range of the measured concentrations in the ML is relatively compacted. Finally, the use of the minimum oxygen concentration to identify the core of the mineralization layer probably includes different water masses but allows us to partly reconcile the Mediterranean stoichiometry with the Redfield value, at least in ML.

In applying the same concept (average ratio vs. linear equation) to DOM and POM, we obtain a broad picture of the stoichiometry inside the two basins or in the Mediterranean Sea (Table 3). In the DOM, high and similar average C:N:P ratios were observed in the western and eastern basins. However, the slopes of the regressions were similar to those observed in the mineral compartment in the western basin, whereas they were lower and close to the Redfield

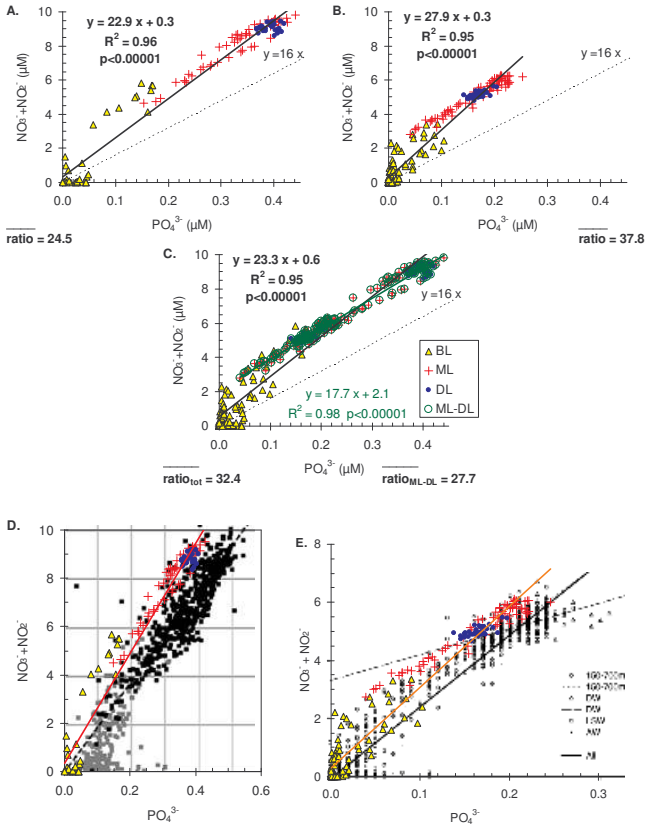

Fig. 8. Plots, linear relationships and probabilities for the slope between $NO_3^- + NO_2^-$ and PO_4^{3-} in **(A)** the western basin, **(B)** the eastern basin, and **(C)** the whole Mediterranean Sea, during the BOUM Cruise. Data are separated for the three layers defined in the text, BL, ML and DL. The Redfield value ($y = 16x$) is indicated by the dashed line. For **(C)**, data for BL have been excluded (ML-DL) to give rise to the second linear equation ($y = 17.7x + 2.1$). The average ratio for data a given at the bottom of each graph. **(D)** Superposition of graph **(A)** and Fig. 2f redraw from Schroeder et al. (2010) (data from the MEDOCC05 survey). **(E)** Superposition of graph **(B)** and Fig. 5 redraw from Kress and Herut (2001) (data from the POEM-Oc91 survey).

values in the eastern basin (Table 3). In POM, it is quite different as the relationships tended towards an ideal elemental co-variation, with an intercept equal to 0, at least for PN:PP. Then the average ratios and regression slopes were similar. When considering the whole water column, the highest ratios were encountered in the western basin, which indicates a POM enriched in C compared to N and P, and in N compared to P. In our study, the C:N:P ratios in the mineral, POM, and DOM pools within the BL largely exceeded the Redfield ratios, as a consequence of the severe deficiency in phosphorus under summer conditions due to biological uptake (Krom et al., 1991). In our data, the deviation from canonical Redfield values was greatest in the DOM > DIM > POM and increased from DL to BL.

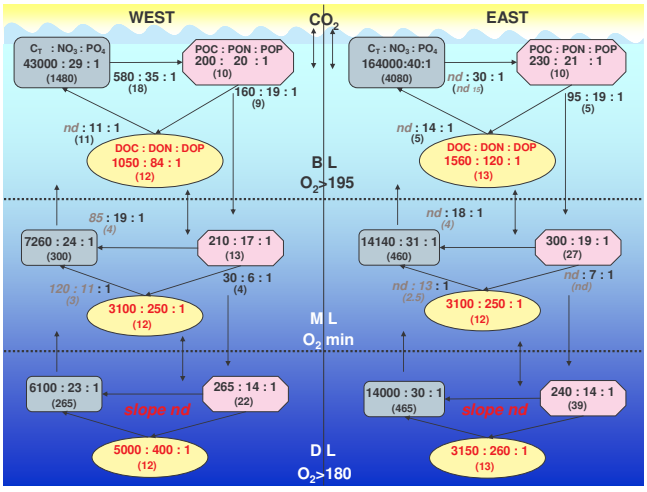

Fig. 9. Representation of the elemental C:N:P stoichiometry in terms of stocks and fluxes for the western (left) and eastern (right) basins of the Mediterranean Sea. The water column is divided in BL, ML and DL as justified in Fig. 2. The blue rectangular boxes with smooth corners symbolize the mineral compartment, the pink rectangular boxes with sharp corners symbolize the POM, whereas the yellow circles symbolize the DOM. In each box, the indicated ratios correspond to the average concentration ratios over the layer for C:P, and N:P. The values in brackets correspond to the average C:N ratio. On arrows, indicated ratios correspond to the slope of the linear regression equations between C:P, and N:P, respectively. The values in brackets correspond to the slope of the C:N plot regression. (nd) is for non significant linear relationship ($\alpha = 0.05$).

4.4 A proposed view for the biogeochemical functioning of the Mediterranean Sea during summer

To summarize our observations, we propose a synthesis of the biogeochemical functioning of the Mediterranean Sea during the 2008 summer period (Fig. 9). In this scheme, the western and the eastern basins are separated and divided in three vertical layers as BL, ML and DL. We assume that the average ratio of two elements represents the stock, and the slope of the linear regression is treated as a first order approximation to the reaction rate ratio, i.e. the net flux resulting from production/consumption processes. We then hypothesize that in BL, the dominant fluxes are from mineral to POM by biological consumption (i.e. the slope of mineral plots), then from POM to DOM by excretion, lyses or grazing (i.e. the slope of POM plots), and from DOM to nutrients by mineralization processes (i.e. the slope of DOM plots). In ML and DL layers, the fluxes are reversed from POM to nutrients because nutrient uptake is supposed to be weak and because the main source of nutrients is the remineralization of sinking biological material from the upper layers (Krom et al., 2010; Schroeder et al., 2010). The link between the three layers is symbolized by the POM downward flux, the upward flux of nutrients and exchange of DOM. We then compare

the functioning of the two basins and the transfer through the water column by considering the Redfield ratios as a reference. BL is characterized by seasonal variability and here represents the summer condition, whereas ML and DL are considered to be less variable and representative of the mean situation of the Mediterranean Sea.

The west-east oligotrophic gradient is again reflected by an increase in the 3 compartments of all C:P and N:P ratios in the BL, although similar ratios in the exchange fluxes are observed (Fig. 9). The vertical distribution of POM was progressively enriched in C relative to N and P, particularly in the ML of the eastern basin. Remineralization of the sinking organic matter is thought to produce a build-up of C relative to N and P, and N relative to P. Our measurements reinforce this view for the western basin and in the ML for the eastern basin, but surprisingly, no increase in N relative to P with depth is seen for the whole of the Mediterranean Sea. Krom et al. (2005) obtained similar results in the eastern basin.

The relative P-depletion is highlighted when considering the DOM pool. The labile and semi-labile DOM fraction can be major sources of C, N, and P for planktonic food webs via bacterial assimilation (Thingstad and Rassoulzadegan, 1995). The DON:DOP ratio increased by a factor 3 from BL to ML (84 to 250) and by a factor 2 from ML to DL (250 to 400) in the western basin and by a factor 2 (120 to 250) from BL to ML in the eastern basin. In the eastern basin, BL showed a stronger P-deficit than in the western basin (DOC:DOP = 1050–1560 and DON:DOP = 84–120 for west-east for similar DOC:DON of 12–13) but reached surprisingly similar stoichiometry in the ML of both basins. Christaki et al. (2011) obtained similar results about this relative west-east homogeneity for biological ecosystem functioning. The authors found a clear west-east gradient in terms of heterotrophic biomass but not in terms of production.

The DOM accumulation usually provides evidence for the refractory nature of DOM pool and P-depletion is a general feature derived from a rapid recycling of the P-rich molecules within DOM (Thingstad and Rassoulzadegan, 1995; Thingstad et al., 2008). In our case, organic phosphorus was consumed in BL and ML of both basins, but only in the DL of western basin indicating that P was recycled faster or more efficiently in the western basin (Fig. 9). It is generally assumed that the same assumption could be applied to the C:N ratio, as N is thought to be recycled faster than C, yet, our data clearly show a noticeable stability of the DOC:DON ratio (12–13) over the whole Mediterranean Sea.

The fact that POM was progressively enriched in C and DOM in C and N undoubtedly indicates that P is the limiting factor of microbial growth in the Mediterranean Sea. Finally, the function of the western basin can be defined using our 3 layers model whereas the eastern basin tends towards a 2 layers structure as ML and DL show very similar partitioning. We consider that the patterns observed during our study are the result of an imbalance and disequilibrium of the allochtonous nutrient loads introduced to the two basins, with greater inputs into the western Mediterranean Sea (Ludwig et al., 2010). Riverine and atmospheric inputs all have N:P ratios that significantly exceed the Redfield ratio in both basins (Conan et al., 2011), and atmospheric deposition is the major external source of bioavailable N to the eastern basin (Krom et al., 2010).

5 Conclusions

This study provides an extensive examination of C, N, P distributions and stoichiometry along a longitudinal transect across the open Mediterranean Sea during the summer period. We have shown that in the Mediterranean Sea, the production of organic matter in the BL (consumption of nutrients) and its mineralization in the deeper layers (ML and DL in the western basin, and ML in the eastern basin) are not necessary far from the Redfield equilibrium in terms of N and P. Indeed, the faster recycling of P compared to N and C explains the seasonal evolution of the intercept in the PO_4^{3-} vs. NO_3^- plot (from about 2 in winter to a negative value at the end of summer). Yet, further work is needed to explore this process, because the rate variability is not sufficient to explain the nonlinearity of the relation in the deepest samples described by Krom et al. (1991).

The western and eastern basins have similar biological functioning. The oligotrophic gradient from West to East could be then attributed to the difference in the allochtonous nutrient sources in terms of quantity and quality (Ribera d'Alcalà et al., 2003; Ludwig et al., 2010; Schroeder, 2010; Krom et al., 2010), and to the specific hydrodynamic features of the Mediterranean Sea (Robinson et al., 2001; Millot and Taupier-Letage, 2005). Crispi et al. (2001) showed that the sole hydrodynamic regime (inverse estuarine circulation) was not sufficient to explain the oligotrophic status. They further suggested that in the long run, the trophic gradient between the western and the eastern Mediterranean was maintained by the biological pump.

As a consequence of the unique nature of the Mediterranean Sea, climate change effects are predicted to play a prominent role in modifying its nutrient status (Marty and Chiavérini, 2010). Our results on the elemental matter partitioning along the west-east Mediterranean gradient of trophic status provide new insights for identifying and understanding the fundamental interactions between marine biogeochemistry and ecosystems, which will ultimately help to predict the impacts of environmental climate changes on the Mediterranean marine ecosystems.

Acknowledgements. This work is a contribution to the BOUM (Biogeochemistry from the Oligotrophic to the Ultraoligotrophic Mediterranean) project financed by the French national LEFE-CYBER program and the European commission SESAME IP. The authors thank the captain and the crews of the R/V *L'Atalante* for outstanding shipboard operations. We really want to thank

A. Murray for her helpful comments and corrections in the English language in the manuscript and the two anonymous reviewers who made a pertinent job.

Edited by: C. Jeanthon

The publication of this article is financed by CNRS-INSU.

References

Anderson, T. R., Hessen, D. O., Elser, J. J., and Urabe, J.: Metabolic stoichiometry and the fate of excess carbon and nutrients in consumers, Am. Nat., 165, 1–15, 2005.

Arrigo, K. R.: Marine microorganisms and global nutrient cycles, Nature, 437, 349–355, 2005.

Béthoux, J.-P. and Copin-Montégut, G.: Phosphorus and nitrogen in the Mediterranean Sea: specificities and forecastings, Oceanol. Acta, 9, 75–78, 1988.

Béthoux, J. P., Morin, P., and Ruiz-Pino, D. P.: Temporal trends in nutrient ratios: chemical evidence of Mediterranean ecosystem changes driven by human activity, Deep-Sea Res. Pt. II, 49, 2007–2015, 2002.

Cauwet, G.: HTCO method for dissolved organic carbon analysis in sea water: influence of catalyst on blank estimation, Mar. Chem., 47, 55–64, 1994.

Cauwet, G.: Determination of dissolved organic carbon (DOC) and nitrogen (DON) by high temperature combustion, in: Methods of seawater analysis, 3rd edn., edited by: Grashoff, K., Kremling, K., and Ehrhard, M., 407–420, 1999.

Christaki, U., Van Wambeke, F., Lefevre, D., Lagaria, A., Prieur, L., Pujo-Pay, M., Grattepanche, J.-D., Colombet, J., Psarra, S., Dolan, J. R., Sime-Ngando, T., Conan, P., Weinbauer, M. G., and Moutin, T.: The impact of anticyclonic mesoscale structures on microbial food webs in the Mediterranean Sea, Biogeosciences Discuss., 8, 185–220, doi:10.5194/bgd-8-185-2011, 2011.

Conan, P., Turley, C. M., Stutt, E., Pujo-Pay, M., and Van Wambeke, F.: Relationship between phytoplankton efficiency and the proportion of bacterial production to primary production in the Mediterranean Sea, Aquat. Microb. Ecol., 17, 131–144, 1999.

Conan, P., Søndergaard, M., Kragh, T., Thingstad, F., Pujo-Pay, M., Williams, P. J. le B., Markager, S., Cauwet, G., Borch, N. H., Evans, D., and Riemann, B.: Partitioning of organic production in marine plankton communities: The effects of inorganic nutrient ratios and community composition on new dissolved organic matter, Limnol. Oceanogr., 52, 753–765, 2007.

Conan, P., Bonnet, S., Guieu, C., Leblanc, K., Van Wambeke F., Pujo-Pay, M., Ghiglione, J.-F, Pulido-Villena, E., Rees, A. P., Jacquet, S. H. M., Ridame, C., Ruiz Pino, D., Sempéré, R., Lefèvre, D., Migon, C., Moutin, T., Sicre, M. A., Tamburini, C., Tanaka, T., and Touratier, F.: Influence of nutrients sources and stoichiometry, Chap. IV, in: White book of Mermex program, https://mermex.com.univ-mrs.fr/, Prog. Oceanogr., in press, 2011.

Crispi, G., Mosetti, R., Solidoro, C., and Crise, A.: Nutrients cycling in Mediterranean basins: the role of the biological pump in the trophic regime, Ecol. Model., 138, 101–114, 2001.

Crombet, Y., Leblanc, K., Quéguiner, B., Moutin, T., Rimmelin, P., Ras, J., Claustre, H., Leblond, N., Oriol, L., and Pujo-Pay, M.: Deep silicon maxima in the stratified oligotrophic Mediterranean Sea, Biogeosciences, 8, 459–475, doi:10.5194/bg-8-459-2011, 2011.

Deutsch, C., Sarmiento, J. L., Sigman, D. M., Gruber, N., and Dunne, J. P.: Spatial coupling of nitrogen inputs and losses in the ocean, Nature, 445, 163–167, 2007.

Diaz, F. and Raimbault, P.: Nitrogen regeneration and dissolved organic nitrogen release during spring in a NW Mediterranean coastal zone (Gulf of Lions): implications for the estimation of new production, Mar. Ecol.-Prog. Ser., 197, 51–65, 2000.

DOE: Handbook of methods for analysis of the various parameters of the carbon dioxide system in seawater; version 2, edited by: Dickson, A. G. and Goyet, C., ORNL/CDIAC-7, 187 pp., 1994.

D'Ortenzio, F. and Ribera d'Alcalà, M.: On the trophic regimes of the Mediterranean Sea: a satellite analysis, Biogeosciences, 6, 139–148, doi:10.5194/bg-6-139-2009, 2009.

Ediger, D. and Yilmaz, A.: Characteristics of deep chlorophyll maximum in the Northeastern Mediterranean with respect to environmental conditions, J. Marine Syst., 9, 291–303, 1996.

Ediger, D., Tugrul, S., and Yilmaz, A.: Vertical profiles of particulate organic matter and its relationship with chlorophyll-a in the upper layer of the NE Mediterranean Sea, J. Marine Syst., 55, 311–326, 2005.

Falkowski, P. G.: Evolution of the nitrogen cycle and its influence on the biological sequestration of CO_2 in the ocean, Nature, 387, 272–275, 1997.

Falkowski, P. G. and Davis, C. S.: Natural proportions, Nature, 431, 131, doi:10.1038/431131a, 2004.

Fanning, K. A.: Nutrient provinces in the Sea: Concentration ratios, reaction rate ratios, and ideal covariation, J. Geophys. Res., 97, 5693–5712, 1992.

Geider, R. J. and La Roche, J.: Redfield revisited: variability of C:N:P in marine microalgae and its biochemical basis, Eur. J. Phycol., 37, 1–17, 2002.

Gruber, N. and Sarmiento, J. L.: Global patterns of marine nitrogen fixation and denitrification, Global Biogeochem. Cy., 11, 235–266, 1997.

Hansell, D. A. and Carlson, C. A.: Biogeochemistry of marine dissolved organic matter, Academic Press, San Diego (USA), 774 pp., 2002.

Herut, B., Krom, M. D., Pan, G., and Mortimer, R.: Atmospheric input of nitrogen and phosphorus to the Southeast Mediterranean: Sources, fluxes, and possible impact, Limnol. Oceanogr., 44, 1683–1692, 1999.

Holmes, M. R., Aminot, A., Kérouel, R., Hooker, B. A., and Peterson, B. J.: A simple and precise method for measuring ammonium in marine and freshwater ecosystems, Can. J. Fish. Aquat. Sci., 56, 1801–1808, 1999.

Ignatiades, L.: Scaling the trophic status of the Aegean Sea, eastern Mediterranean, J. Sea Res., 54, 51–57, 2005.

Karl, D. M., Björkman, K. M., Dore, J. E., Fujieki, L., Hebel, D. V., Houlihan, T., Letelier, R. M., and Tupas, L. M.: Ecological

nitrogen-to-phosphorus stoichiometry at station ALOHA, Deep-Sea Res. Pt. II, 48, 1529–1566, 2001.

Klausmeier, C., Litchman, E., Daufresne, T., and Levin, S.: Phytoplankton stoichiometry, Ecol. Res., 23, 479–485, 2008.

Klein, B., Roether, W., Kress, N., Manca, B. B., Ribera d'Alcala, M., Souvermezoglou, E., Theocharis, A., Civitarese, G., and Luchetta, A.:, Accelerated oxygen consumption in eastern Mediterranean deep waters following the recent changes in thermohaline circulation, J. Geophys. Res., 108(C9), 8107, , 2003.

Kress, N. and Herut, B.: Spatial and seasonal evolution of dissolved oxygen and nutrients in the Southern Levantine Basin (Eastern Mediterranean Sea): chemical characterization of the water masses and inferences on the N : P ratios, Deep-Sea Res. Pt. I, 48, 2347–2372, 2001.

Krom, M. D., Kress, N., Brenner, S., and Gordon, L. I.: Phosphorus limitation of primary productivity in the eastern Mediterranean Sea, Limnol. Oceanogr., 36, 424–432, 1991.

Krom, M. D., Woodward, E. M. S., Herut, B., Kress, N., Carbo, P., Mantoura, R. C. F., Spyres, G., Thingstad, T. F., Wassmann, P., Wexels-Riser, C., Kitidis, V., Law, C. S., and Zodiatis, G.: Nutrient cycling in the south east Levantine basin of the eastern Mediterranean: Results from a phosphorus starved system, Deep-Sea Res. Pt. II, 52, 2879–2896, 2005.

Krom, M. D., Emeis, K. C., and Van Cappellen, P.: Why is the Eastern Mediterranean phosphorus limited?, Prog. Oceanogr., 85, 236–244, 2010.

Lefèvre, D., Minas, H. J., Minas, M., Robinson, C., Williams, P. J. L., and Woodward, E. M. S.: Review of gross community production, primary production, net community production and dark respiration in the gulf of Lions, Deep-Sea Res. Pt. II, 44, 801–832, 1997.

Lomas, M. W. and Lipschultz, F.: Forming the primary nitrite maximum: Nitrifiers or phytoplankton? Limnol. Oceanogr., 51, 2453–2467, 2006.

Lucea, A., Duarte, C. M., Agusti, S., and Sondergaard, M.: Nutrient (N, P and Si) and carbon partitioning in the stratified NW Mediterranean, J. Sea Res., 49, 157–170, 2003.

Ludwig, W., Bouwman, A. F., Dumont, E., and Lespinas, F.: Water and nutrient fluxes from major Mediterranean and Black Sea rivers: past and future trends and their implications for the basin-scale budgets, Global Biogeochem. Cy., 24, GB0A13, doi:10.1029/2009GB003594, 2010.

Lutz, M., Dunbar, R., and Caldeira, K.: Regional variability in the vertical flux of particulate organic carbon in the ocean interior, Global Biogeochem. Cy., 16, 1037, doi:10.1029/2000GB001383, 2002.

Marty, J. C. and Chiavérini, J.: Hydrological changes in the Ligurian Sea (NW Mediterranean, DYFAMED site) during 1995–2007 and biogeochemical consequences, Biogeosciences, 7, 2117–2128, doi:10.5194/bg-7-2117-2010, 2010.

Mc Gill, D. A.: The relative supplies of phosphate, nitrate and silicate in the Mediterranean Sea, Rapport des Procès Verbaux des Réunions de la CIESM, XVIII, 737–744, 1965.

Mermex group: White book of Mermex program, https://mermex.com.univ-mrs.fr/, Prog. Oceanogr., in press, 2011.

Millot, C. and Taupier-Letage, I.: Circulation in the Mediterranean Sea, in: The Mediterranean Sea, The Handbook of Environmental Chemistry, Springer Berlin/Heidelberg, 29–66, 2005.

Millot, C., Candela, J., Fuda, J.-L., and Tber, Y.: Large warming and salinification of the Mediterranean outflow due to changes in its composition, Deep-Sea Res. Pt. I, 53, 656–666, 2006.

Moutin, T., Van Wambeke, F., and Prieur, L.: Introduction to the Biogeochemistry from the Oligotrophic to the Ultraoligotrophic Mediterranean experiment: the BOUM program, Biogeosciences Discuss., in preparation, 2011.

Pahlow, M. and Riebesell, U.: Temporal trends in deep ocean Redfield ratios, Science, 287, 831–833, 2000.

Patara, L., Pinardi, N., Corselli, C., Malinverno, E., Tonani, M., Santoleri, R., and Masina, S.: Particle fluxes in the deep Eastern Mediterranean basins: the role of ocean vertical velocities, Biogeosciences, 6, 333–348, doi:10.5194/bg-6-333-2009, 2009.

Paulmier, A. and Ruiz-Pino, D.: Oxygen minimum zones (OMZs) in the modern ocean, Prog. Oceanogr., 80, 113–128, 2009.

Pujo-Pay, M. and Conan, P.: Seasonal variability and export of Dissolved Organic Nitrogen in the North Western Mediterranean Sea, J. Geophys. Res., 108, 1901–1911, 2003.

Pujo-Pay, M. and Raimbault, P.: Improvement of the wet-oxydation procedure for simultaneous determination of particulate organic nitrogen and phosphorus collected on filters, Mar. Ecol.-Prog. Ser., 105, 203–207, 1994.

Pujo-Pay, M., Conan, P., and Raimbault, P.: Excretion of dissolved organic nitrogen by phytoplankton assessed by wet oxidation and N-15 tracer procedures, Mar. Ecol.-Prog. Ser., 153, 99–111, 1997.

Prieur, L. and Sournia, A.: "Almofront-1" (April–May 1991): an interdisciplinary study of the Algeria-Oran geostrophic front, SW Mediterranean Sea, J. Marine Syst., 5, 187–203, 1994.

Redfield, A. C.: On the proportions of organic derivations in sea water and their relation to the composition of plankton, in: James Johnstone Memorial Volume, edited by: Daniel, R. J., University Press of Liverpool, Liverpool, 177–192, 1934.

Redfield, A. C., Ketchum, B. H., and Richards, F. A.: The influence of organisms on the composition of sea water, in: The Sea, ideas and observations on progress in the study of the seas, edited by: Hill, M. N., Interscience, New-York, 29–77, 1963.

Ribera d'Alcalà, M., Civitarese, G., Conversano, F., and Lavezza, R.: Nutrient ratios and fluxes hint at overlooked processes in the Mediterranean Sea, J. Geophys. Res., 108(C9), 8106, doi:10.1029/2002jc001650, 2003.

Robinson, A. R., Wayne, G., Theocharis, A., and Lascaratos, A.: Mediterranean Sea circulation, in: Encyclopedia of Ocean Sciences, edited by: Steele, J., Turekian, K., and Thorpe, S., Academic Press, 2001.

Roether, W., Klein, B., Manca, B. B., Theocharis, A., and Kioroglou, S.: Transient Eastern Mediterranean deep waters in response to the massive dense-water output of the Aegean Sea in the 1990s, Prog. Oceanogr., 74, 540–571, 2007.

Sarmiento, J. L. and Gruber, N.: Ocean Biogeochemical Dynamics, Princeton University Press, Princeton, NJ, 526 pp., 2006.

Schroeder, K., Gasparini, G. P., Borghini, M., Cerrati, G., and Delfanti, R.: Biogeochemical tracers and fluxes in the Western Mediterranean Sea, spring 2005, J. Marine Syst., 80, 8–24, 2010.

Sterner, R. W., Andersen, T., Elser, J. J., Hessen, D. O., Hood, J. M., McCauley, E., and Urabe, J.: Scale-dependent carbon: nitrogen: phosphorus stoichiometry in marine and freshwaters, Limnol. Oceanogr., 53, 1169–1180, 2008.

Sugimura, Y. and Suzuki, Y.: A high temperature catalytic oxydation method for the determination of non-volatile dissolved

organic carbon in sea water by direct injection of a liquid sample, Mar. Chem., 24, 105–131, 1988.

Thingstad, T. F. and Rassoulzadegan, F.: Nutrient limitations, microbial food webs and "biological C-pumps" : suggested interactions in a P-limited Mediterranean, Mar. Ecol.-Prog. Ser., 117, 299–306, 1995.

Thingstad, T. F., Krom, M. D., Mantoura, R. F. C., Flaten, G. A. F., Groom, S., Herut, B., Kress, N., Law, C. S., Pasternak, A., Pitta, P., Psarra, S., Rassoulzadegan, F., Tanaka, T., Tselepides, A., Wassmann, P., Woodward, E. M. S., Riser, C. W., Zodiatis, G., and Zohary, T.: Nature of phosphorus limitation in the ultraoligotrophic eastern Mediterranean, Science, 309, 1068–1071, 2005.

Thingstad, T. F., Bellerby, R. G. J., Bratbak, G., Borsheim, K. Y., Egge, J. K., Heldal, M., Larsen, A., Neill, C., Nejstgaard, J., Norland, S., Sandaa, R. A., Skjoldal, E. F., Tanaka, T., Thyrhaug, R., and Topper, B.: Counterintuitive carbon-to-nutrient coupling in an Arctic pelagic ecosystem, Nature, 455, 387–390, doi:10.1038/nature07235, 2008.

Tréguer, P. and Le Corre, P.: Manuel d'analyses des sels nutritifs dans l'eau de mer, Laboratoire d'Océanographie Chimique, Université de Bretagne Occidentale, Brest, 110 pp., 1975.

Turley, C. M.: The changing Mediterranean Sea – a sensitive ecosystem, Prog. Oceanogr., 44, 387–400, 1999.

Tyrrell, T. and Lucas, M. I.: Geochemical evidence of denitrification in the Benguela upwelling system, Cont. Shelf Res., 22, 2497–2511, 2002.

Van Wambeke, F., Christaki, U., Giannakourou, A., Moutin, T., and Souvemerzoglou, K.: Longitudinal and vertical trends of bacterial limitation by phosphorus and carbon in the Mediterranean sea, Microb. Ecol., 43, 119–133, 2002.

Vidal, M., Duarte, C. M., and Agustí, S.: Dissolved organic nitrogen and phosphorus pools and fluxes in the central Atlantic Ocean, Limnol. Oceanogr., 44, 106–115, 1999.

Wood, E. D., Armstrong, F. A., and Richards, F. A.: Determination of nitrate in sea water by cadmium copper reduction to nitrite, J. Mar. Biol. Assoc. UK, 47, 23–31, 1967.

Zehr, J. P. and Ward, B. B.: Nitrogen cycling in the ocean: New perspectives on processes and paradigms, Appl. Environ. Microb., 68, 1015–1024, doi:10.1128/aem.68.3.1015-1024.2002, 2002.